Water-Soluble Dendritic Architectures with Carbohydrate Shells for the Templation and Stabilization of Catalytically Active Metal Nanoparticles

Michael Krämer,[†,‡] Nelly Pérignon,[†] Rainer Haag,[*,‡,§] Jean-Daniel Marty,[*,†] Ralf Thomann,[‡] Nancy Lauth-de Viguerie,[†] and Christophe Mingotaud[†]

IMRCP, UMR CNRS 5623, Université Paul Sabatier, 118 route de Narbonne, 31062 Toulouse, France; Freiburger Materialforschungszentrum und Institut für Makromolekulare Chemie, Universität Freiburg, Stefan-Meier-Str. 21, 79104 Freiburg, Germany; and Department of Chemistry, Free University of Berlin, Takustrasse 3, 14195 Berlin, Germany

Received May 26, 2005; Revised Manuscript Received July 18, 2005

ABSTRACT: Hyperbranched poly(ethylenimine) (PEI) with amino groups or carbohydrate terminal groups have been used as support materials for metal nanoparticles (i.e., Cu, Ag, Au, and Pt) in water. Various parameters have been optimized, such as pH, concentration of the polymer in solution, and [metal ions]/[polymer] ratio in order to obtain stable metal nanoparticles with a narrow size distribution. TEM measurements revealed that particles with a diameter as low as 1.4 nm were obtained. An increase of stability was obtained after functionalization of PEI with glycidol, gluconolactone, or lactobionic acid. In the case of Pt the catalytical activity of the corresponding nanoparticles was evidenced.

Introduction

Metal nanoparticles are of special interest because they show physical properties owing to quantum-mechanical rules that are neither those of the bulk metal nor those of molecular compounds. Encapsulated metal nanoparticles have found potential application in catalysis[1−5] or material sciences[6] due to their large surface/volume ratio as discussed in the literature.[7] Furthermore, they have also found applications in medicine and biology as labeling agents,[8] for transfer of drugs including genetic material to the nucleus,[9] detection of metal ions in solution,[10] single molecule spectroscopy,[11] and as organic−inorganic semiconductor composites with defined sizes that are promising candidates for nanoelectronic devices.[12]

In the present state of the research, the preparation of nanosized water-soluble analogues of heterogeneous catalysts for the use as more efficient and environmental friendly catalytic systems is still a challenge,[13] and new efficient approaches are required to obtain structures that are stable toward shear forces and dilution. To reach such a goal, the requirements are (a) the development of nanoreactors in which the catalytic nanoparticles can be formed in a controlled fashion (i.e., with an average diameter usually less than 10 nm) and (b) the use of stabilizers which prevent the thermodynamically favored aggregation of the nanoparticles in the solution without any loss of the catalytic properties due to a too strong adsorption of the stabilizers on the active sites of the particles.[14] To overcome these problems, various molecular systems were reported to stabilize metal nanoparticles in aqueous media, such as polyelectrolytes or block copolymers.[15−18] Derivatives of polyamidoamine (PAMAM) dendrimers were often used as nanoreactor and stabilizer for metal nanoparticles.[2,19−26] In contrast to those perfectly branched monodisperse dendrimers, randomly branched polymers can be easily accessible.[27,28] These hyperbranched polymers have already been successfully used as templates for metal nanoparticles.[15,29−32] In the literature, it was suggested that hyperbranched polyamines, e.g. polyethylenimine (PEI), are better suited for stabilization of metal nanoparticles due to the more globular structure as compared to linear polymers.[15] So far poly(ethylene glycol)-functionalized PEIs[15,16] and alkyl-modified PEIs[29,33,34] have been reported as stabilizers for metal nanoparticles in organic solvents.

In this paper, we report for the first time on readily accessible water-soluble dendritic core−shell architectures and study the influence of the attached carbohydrate shell on the formation and stabilization of metal nanoparticles in water. The control of the 3D architecture of the hyperbranched polymer (via choice of the M_w of the polymer and functionalization) might allow size control of the nanoparticles and the enhancement of their stability. For this purpose, three different carbohydrates acting as a shell, i.e., glycidol, gluconolactone, and lactobionic acid, were attached to hyperbranched PEI of different molecular weights (M_w) to obtain the corresponding PEI−glycol, PEI−gluconamide, and PEI−lactobionamide. Various parameters such as pH, concentration, [metal ions]/[polymer] ratio, and the nature of the metal precursors ($HAuCl_4$, $AgNO_3$, $CuSO_4$, and H_2PtCl_6) have been optimized to obtain stable nanoparticle systems. In the case of stabilized Pt nanoparticles, we have also briefly investigated their catalytic activity.

Results and Discussion

Synthesis of Dendritic PEIs with Carbohydrate Shells. Hyperbranched PEIs can be obtained in a single cationic polymerization step of aziridine.[35−37] Slow monomer addition allows control over the degree of branching (DB) as discussed in the literature.[38] These polymers are available in a multigram scale and high molar mass with a polydispersity index typically below

[†] Université Paul Sabatier.
[‡] Universität Freiburg.
[§] Free University of Berlin.
* Corresponding authors. E-mail: marty@chimie.ups-tlse.fr; haag@chemie.fu-berlin.de.

10.1021/ma0510791 CCC: $30.25
Published on Web 08/27/2005

Scheme 1. Structure of Hyperbranched Polymers. Functionalization of PEI with (a) Glycidol (PEI$_x$GLY), (b) Gluconic Acid (PEI$_x$GLU), and (c) Lactobionic Acid (PEI$_x$LAC)

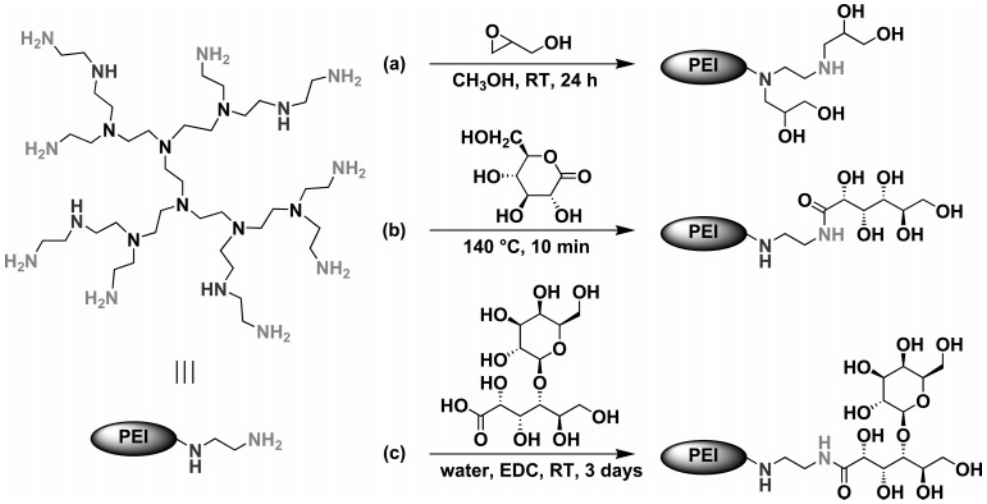

2.0 (Supporting Information).[28] In the following, modified PEIs are labeled as PEI$_x$ with $\times 10^3 = M_w$. In a second reaction step, PEI$_x$ was modified with a covalently attached hydrophilic shell to create water-soluble core−shell architectures with PEI$_x$ as core and the carbohydrate acting as a shell (Scheme 1). The density and size of the shell were varied by functionalization of the amine groups with a controlled amount of glycidol (PEI$_x$GLY), gluconolactone (PEI$_x$GLU), or lactobionic acid (PEI$_x$LAC).

Functionalization with glycidol, leading to PEI$_{25}$GLY (PEI-glycol, Scheme 1a), can be achieved via addition of DL-glycidol to a solution of PEI$_{25}$ in methanol, resulting in complete conversion of the reactive epoxide group after 24 h at room temperature. The degree of functionalization (DF = number of shell molecules/number of monomer unit of PEI, given in %) was determined via integration of the respective ^{1}H NMR signals (Supporting Information). The attachment of D-glucono-1,5-lactone to PEI$_x$ with different M_w (x = 0.8, 5, 21, or 25), leading to PEI$_x$GLU (PEI-gluconamide, Scheme 1b), can be realized in DMSO as reported in the literature with PAMAM dendrimers[39,40] or via a newly developed pathway by a simple melt reaction of glucono-1,5-lactone with PEI$_x$ at 140 °C (see Experimental Section). The advantage of the latter reaction is that only stoichiometrical amounts of water have to be added (gluconolactone:water = 1:1) to obtain a soluble polymer with a precise stoichiometry control. Inverse gated ^{13}C NMR in DMSO indicates that about 70% of the gluconolactone is covalently attached and about 30% is linked via an ionic bridge. Functionalization of the reactive primary and secondary nitrogen atoms of PEI$_x$ with gluconolactone could be realized up to 50% as determined by elemental analysis (Supporting Information). The degree of functionalization controlled by the stoichiometry of the reaction in the case of the PEI$_x$GLU was confirmed by elemental analysis. A higher degree of functionalization via the melt reaction route resulted in a dark brown and insoluble polymer. In the case of the functionalization of PEI$_{25}$ with lactobionic acid, leading to PEI$_{25}$LAC (PEI−lactobionamide, Scheme 1c), 1-ethyl-3-[3-(dimethylamino)propyl]carbodiimide hydrochloride (EDC) was used as coupling reagent in water, and the degree of functionalization was determined via elemental analysis (Supporting Information). The characteristics of the water-soluble polymers are summarized in Table 1.

Table 1. Properties of Investigated Polymers PEI$_x$, PEI$_{25}$GLY, PEI$_x$GLU, and PEI$_{25}$LAC[a]

	M_w [g mol^{-1}]	M_n [g mol^{-1}]	MWD	DP$_n$[c]	DF [%]
PEI$_{0.8}$	800	600	1.3	14	
PEI$_5$	5 000	3 600	1.4	84	
PEI$_{21}$	21 000	10 500	2	244	
PEI$_{25}$	25 000	9 600[b]	2.6	223	
PEI$_{0.8}$GLU	1 800	1 400	1.3	14	33
PEI$_5$GLU	11 900	8 500	1.4	84	33
PEI$_{21}$GLU	51 200	25 600	2	244	33
PEI$_{25}$GLU	59 800	23 000	2.6	223	33
PEI$_{25}$GLY	47 800	18 400	2.6	223	53
PEI$_{25}$LAC	78 000	30 000	2.6	223	27

[a] GLU = functionalization with gluconic acid. GLY = functionalization with glycidol. LAC = functionalization with lactobionic acid. M_n = number-averaged molar mass. M_w = mass-averaged molar mass. MWD = molecular weight dispersity. DP$_n$ = number degree of polymerization. DF = degree of functionalization of all monomer units (Supporting Information). [b] M_n = 9600 g mol^{-1} calculated from M_w and MWD is too low; a M_n of 12 000 g mol^{-1} can be estimated from GPC due to existence of a shoulder in the diagram. [c] Represents also the number of primary and tertiary amine groups of the hyperbranched structure.

Preparation of Metal Nanoparticles. Polymer-stabilized nanoparticles were prepared in a two-step process. After complexation of metal ions with the respective polymer in a first step, a chemical reduction with sodium borohydride was performed in a second step to obtain the metal nanoparticles.

Complexation with Metal Cations. In the case of dendrimers, it was shown in the literature that they can only encapsulate a maximum number of metal ions per molecule.[21] The maximum metal loading of the dendrimer and the value of the [metal ions]/[dendrimer] ratio determines the size of the formed nanoparticles.[23] To evaluate the ability of the dendritic architecture of various PEIs to act in the same fashion as dendrimers, complexation properties of PEI$_5$ and PEI$_5$GLU were determined in the case of copper, gold, and platinum ions. (Because of rapid self-reduction of silver ions in the presence of polymers prior to the addition of a reduction agent, complexation studies could not be rigorously performed in the case of silver.) All the complexation results obtained are summarized in Table 2. In the case of Pt(IV) and Au(III), slow kinetics have

Table 2. Complexation Properties of PEI_5 and PEI_5GLU[a]

	PEI_5	PEI_5GLU
$CuSO_4$	40	40
H_2PtCl_6	45	40
$HAuCl_4$	35	40

[a] Precision on values is ±5.

been reported for complexation with dendrimers.[1] To avoid any problems, the incubation time for metal uptake was chosen to be equal to 48 h for all metals, although due to the lower degree of branching, complexation with hyperbranched polymers should occur more rapidly. (No significant evolution of the spectra was observed 24 h after the beginning of the complexation process.) All samples were stable on this time scale if protected from light exposure.

Initially, an aqueous solution of the respective polymer (at various concentrations calculated with the M_w value) was mixed with an aqueous solution of metal ions ($CuSO_4$, $HAuCl_4$, H_2PtCl_6, or $AgNO_3$) to obtain a controlled molar ratio [metal ions]/[polymer] (in the range 0−100). Figure 1 shows the results obtained from complexation of copper ions with PEI_5. In the absence of a polymer with complexation capabilities, Cu^{II} exists primarily as $[Cu(H_2O)_6]^{2+}$ in aqueous solutions, which gives rise to a broad, weak absorption band at 810 nm associated with a d−d transition ($\epsilon \sim 10$). In the presence of hyperbranched PEI_5, λ_{max} for the Cu^{II} d−d transition was shifted to 605 nm ($\epsilon \sim 30$). In addition, a strong ligand-to-metal charge-transfer (LMCT) transition appeared at 300 nm (Figure 1A). This change in the UV−vis spectrum allows to follow the Cu^{II} ion complexation with different polymers. The absorbance at λ_{max} increased with the $[Cu^{II}]$/[polymer] ratio (Figure 1B) until a critical value is reached, above which the absorbance increased only slowly. The change in the slopes suggests different environments for the copper cations before and after this critical value and therefore some interactions between the nitrogen atoms of the polymer and the metal cations. Extrapolating the two linear regions of the absorbance at this wavelength allows to evaluate the maximum copper loading of the polymer. This analysis indicates that PEI_5 (hyperbranched polyethylenimine with $M_w = 5000$ g mol^{-1}) can complex up to 40 Cu^{II} ions. Functionalization of the primary or secondary amino groups with gluconamide results in similar observations, indicating that the two polymers (PEI_5 and PEI_5GLU) possess the same complexation capabilities.

In the case of $HAuCl_4$, besides a very weak band around 640 nm, the absorption spectrum of a $HAuCl_4$ solution exhibits a strong absorption band at 226 nm and a shoulder at 290 nm due to charge transfer between the metal and the chloro ligands (Supporting Information). After addition of $HAuCl_4$ to a solution of PEI_5, the absorbance at 290 nm increased linearly with the quantity of added Au^{III} ions until the $[Au^{III}]$/[PEI] ratio reaches ca. 35. The change in the slopes suggests also some interactions between the nitrogen atoms of the polymer and the gold cations. As already described in the case of chitosan,[41] formation of ion pairs between $AuCl_4^-$ or hydrolyzed forms ($AuCl_3OH^-$, etc.) and the protonated amino groups of PEI could be responsible at least partially for this phenomenon. Whatever the nature of the interaction between $AuCl_4^-$ and the hyperbranched polymer may be, this experiment indicates that PEI_5 can be loaded with a maximum number of ca. 35 Au^{III} ions per macromolecule and PEI_5GLU with ∼40 Au^{III} ions per macromolecule.

In the absence of PEI_5 or PEI_5GLU, the UV−vis absorption spectrum of a 10^{-4} M H_2PtCl_6 solution consists of a strong absorption peak at 196 nm arising from a ligand-to-metal charge-transfer transition (Supporting Information). If PEI_5 or PEI_5GLU is added to this solution, a new band at 230 nm emerges while the band at 196 nm shifts slightly to 199 nm. The absorbance at 230 nm is proportional to the number of complexed Pt^{IV} ions by the polymer over the range of $[Pt^{IV}]/[PEI_5GLU] = 0-40$, which indicates that it is possible to control the extent of the complexation by the $[Pt^{IV}]/[PEI_5]$ and $[Pt^{IV}]/[PEI_5GLU]$ ratio.

These results demonstrate that loading of the dendritic architectures by metal cations is possible in a well-defined range, as it was already observed for dendrimers. The maximum number of loaded metal ions was found to be around 40 for PEI_5 and is close to the number evaluated for a fourth-generation PAMAM dendrimer (i.e., 50),[32] whereas the molecular weight of the hyperbranched polymer is only half of it. This suggests, as already observed with hyperbranched polymers derivated from PAMAM dendrimers,[32] that the open structure of the hyperbranched polymer compared to the dendrimer architecture facilitates the interactions of the metal ions with the internal chemical functions, increasing therefore the maximum load of ions per polymer. Moreover, the substitution of amino groups of PEI_5 by gluconamide did not significantly modify the complexation properties. This suggested a possible interaction between substituted amino groups and metal ions (or only the dendritic N atoms are involved in the complexation process).

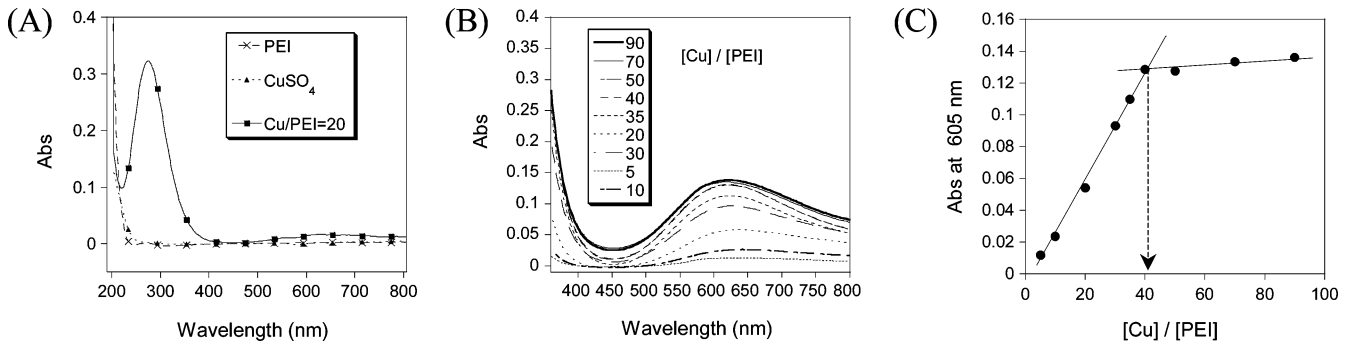

Figure 1. (A) Absorption spectra of aqueous solutions: 2×10^{-4} mol L^{-1} of $CuSO_4$; 10^{-5} mol L^{-1} of PEI_5; 2×10^{-4} mol L^{-1} of $CuSO_4$, and 10^{-5} mol L^{-1} of PEI_5. (B) Absorption spectra of a solution 5×10^{-5} mol L^{-1} of PEI_5 with various amounts of Cu^{II} (the optical path length is 0.5 cm). (C) Absorbance at 605 nm as a function of [copper ion]/[polymer] ratio. Determination of capacity was based on the highest achieved absorbance.

Formation of Nanoparticles: Conditions of Stabilization. To obtain the respective metal nanoparticles, reduction of the cations complexed by the polymer was carried out with a 1−100 fold excess of $NaBH_4$. If not mentioned, a 100-fold excess was chosen to induce a fast reduction of the metal cations. Numerous publications deal with the formation, stability, and size of metal nanoparticles in dependence of the [metal ions]/[polymer] ratio,[15,16,19,20] pH of the solution,[15,42] concentration of the polymer in solution,[17−20] concentration of metal cations in solution,[17] and the reduction agent applied.[15,16] In the following part, parameters that influence the stability of nanoparticles/PEI systems, such as the [metal ions]/[polymer] ratio, the molecular weight of the polymer core, pH of the solutions, and the concentration of the polymer in solution, were investigated.

Stability Depending on the Concentration of the Polymer and the [Metal ions]/[Polymer] Ratio. In a first set of experiments, the influence of the polymer concentration in solution on the stability of metal nanoparticles and the maximum possible [metal ions]/[polymer] ratio was evaluated in order to obtain systems that show no sign of immediate precipitation after reduction by sodium borohydride. For concentrated polymer solutions (10^{-2} and 10^{-3} mol L^{-1}) immediate complete or partial precipitation was observed regardless of the [metal ions]/[polymer] ratio. In the case of lower concentrations of the polymers (10^{-4}−10^{-5} mol L^{-1}), immediate precipitation was observed only for [metal ions]/[polymer] ratio above the maximum complexation numbers given in Table 2. Under these conditions, copper and silver nanoparticles were less stable than their gold and platinum counterparts: partial or even complete reoxidation of metal nanoparticles was observed when exposed to atmospheric oxygen as expected[22] (Supporting Information). With these results in mind, hyperbranched polymer solutions with concentrations in the range of 10^{-4}−10^{-5} mol L^{-1} should result in the most stable metal nanoparticles with [metal ions]/[polymer] ratios below 40 if high molecular weight polymers are used. The observation of increased stability of nanoparticles at lower concentrations of the stabilizer in aqueous solution is in agreement with the literature.[43]

Stability of Metal Nanoparticles in Dependence of the pH. To evaluate the influence of the pH on the stability of metal nanoparticles, the more stable Au nanoparticles were investigated to minimize the influence of the polymer−metal system. The primary effect of excess borohydride was to reduce the metal ions, but at the same time it raises the pH of the solution, so it was necessary to adjust the pH with buffer solution. The Au^{III} compound and $PEI_{21}GLU$ were mixed together to obtain an aqueous solution with a concentration of 230 and 9.1 μmol L^{-1}, respectively, resulting in a [metal ions]/[polymer] ratio of 25. The pH of the solution was adjusted with a buffer solution to obtain pH values of 2, 5, 8, and 12. Only in the case of pH = 12 were stable nanoparticles obtained; in all other cases precipitation occurred after reduction. The increased stability of gold nanoparticles after reduction with $NaBH_4$ at a pH of 12 is in agreement with the literature[15,16] and was also observed for other metal nanoparticles such as Pd, Pt, and Au and PEI−PEG stabilizers. All further experiments were therefore carried out in buffered solution at a pH of 12.

Table 3. Gold Nanoparticles Obtained from Different Metal Loading [Au^{III}]/[Polymer] Ratios[a]

sample	M_w [g mol^{-1}]	M_n [g mol^{-1}]	stability	ratio [Au^{III}]/[polymer]
$PEI_{0.8}$	800	600	precipitation	0.67
			precipitation	3.3
			precipitation	6.7
$PEI_{0.8}GLU$	1 800	1 400	precipitation	0.74
			precipitation	3.7
			precipitation	7.4
PEI_5	5 000	3 600	stable[b]	6.8
PEI_5GLU	6 900	8 500	stable[c]	6.8
PEI_{21}	21 000	10 500	stable	5.0
$PEI_{21}GLU$	51 200	25 600	stable	5.0

[a] pH of all solutions was 12 adjusted with phosphate buffer; concentration of $HAuCl_4$ was 0.29 mmol L^{-1}; reduction was carried out with $NaBH_4$; concentration of the polymer was between 0.4 and 0.06 mmol L^{-1}. [b] Partial precipitation was observed immediately. [c] Partial precipitation was observed after 1 week.

Stability in Dependence of the Molecular Weight of the Polymeric Core. To investigate the influence of the molecular weight of the polymer on the stabilization properties, three different PEIs ($PEI_{0.8}$, PEI_5, and PEI_{21}) functionalized with gluconic acid were synthesized. Additionally, the stability of gold nanoparticles was investigated with unfunctionalized PEI_x (Table 3). Higher molecular weight polymers have been found to be better suited to stabilize higher [metal ions]/[polymer] ratios independent of the nature of the attached shell. No stabilization was possible with PEIs with a molecular weight of 800 g mol^{-1} regardless if they were functionalized with gluconic acid or not. However, gold nanoparticles can be stabilized with high molecular weight unfunctionalized PEI (see Table 3, PEI_{21}). For the intermediate case (i.e., PEI_5), the solution was filtrated after reduction due to partial precipitation of gold which occurred immediately. In contrast, the PEI_5GLU showed only partial precipitation after 1 week.

Influence of the Attached Carbohydrate Chain on the Stability. To enhance the stability of nanoparticles, the influence of an attached carbohydrate chain on the stabilization properties of the polymers on silver nanoparticles at a pH of 12 was examined. Previous experiments revealed that silver nanoparticles were less stable than their gold counterparts and therefore more sensitive to the nature of the applied stabilizer. Functionalization of the linear and terminal monomer units of PEI_{25} with glycidol (53%), gluconolactone (33%), and lactobionic acid (27%) results in the desired polymers with PEI core and carbohydrate shell. Experimentally, even the higher degree of functionalization of PEI with glycidol (53%) results in reduced stability compared to PEI functionalized with gluconolactone (33%). The rather short glycol units are therefore not sufficient to enhance stability of the silver nanoparticles. The attachment of the more bulky lactobionic acid (27%) results in a further increase of stability as compared to the gluconamide. The degree of functionalization with lactobionic acid is comparable to the PEI−gluconamide. However, none of the polymers were able to stabilize silver nanoparticles for more than 2 weeks regardless of their functionalization. Nevertheless, a clear increase in stability with increasing shell size was revealed. These experiments demonstrate that the stability increased in the series glycol < gluconamide < lactobionamide.

Table 4. Size of Different Metal Nanoparticles Stabilized with Different Polymers in Dependence of the [Metal Ions]/[Polymer] Ratio[a]

		size [nm] ± standard deviation ([metal ions]/[polymer] ratio)		
PEI	functionalization	Ag	Au	Pt[b]
PEI_5		13.7 ± 12.6 (8.5)	8.8 ± 3.0 (6.8)	40 ± 10 (20)[c]
PEI_5	GLU	6.4 ± 5.6 (8.5)	7.7 ± 2.6 (6.8)	8.6 ± 1.6 (20)
PEI_{21}		10.7 ± 7.6 (6.3)	6.3 ± 5.3 (5)	
PEI_{21}	GLU	1.9 ± 0.6 (6.4)	1.3 ± 0.3 (5)	
PEI_{25}		15.7 ± 5.6 (23.6)	4.1 ± 2.3 (25)	
PEI_{25}	GLU	13.6 ± 6.4 (23.6)	4.2 ± 3.3 (25)	
PEI_{25}	GLY	12.8 ± 6.5 (25.5)	3.8 ± 1.6 (25)	
PEI_{25}	LAC	12.6 ± 9.2 (25.7)	5.6 ± 4.5 (25)	

[a] GLU = functionalization with gluconolactone (33%). GLY = functionalization with glycidol (53%). LAC = functionalization with lactobionic acid (27%). [b] In contrast to the Ag and Au nanoparticles, the pH was controlled via the addition of $NaBH_4$. [c] Very polydisperse sample with large clusters (more than 100 nm).

Concerning stability, the experiments performed so far revealed that the use of high pH conditions and [metal ions]/[polymer] ratio below maximum load numbers are necessary conditions to stabilize metal nanoparticles with PEI derivatives in water. Nevertheless, when considering other parameters, differences in stability were apparently dependent on the nature of the metal nanoparticle. No stabilization was possible in conjunction with copper particles. Reoxidation occurs immediately in the presence of oxygen, which is in agreement with the literature.[21] Silver nanoparticles were less stable than their gold counterparts. The experiments revealed that the stability of silver nanoparticles depends on the polymer applied for stabilization and can be extended with functionalized PEI_x (PEI_xGLU and PEI_xLAC). Gold nanoparticles could be stabilized with unfunctionalized PEI_x; however, smaller particles were obtained if the PEI_xGLU was used. Pt particles were stable for months if PEI_xGLU was used. They could not be stabilized with unfunctionalized PEI.

Formation of Nanoparticles: Size Control of the Nanoparticles Obtained. The effects of [metal ions]/[polymer] ratio, molar mass, and nature of the carbohydrate shell on the size of the nanoparticles formed are investigated. PEI_x with different M_w (PEI_5, PEI_{21}, and PEI_{25}) was functionalized with various carbohydrate shells. The resulting polymers PEI_5GLU, PEI_{21}GLU, PEI_{25}GLU, PEI_{25}GLY, and PEI_{25}LAC were used to create the respective nanoparticles. The results obtained from the analysis of TEM measurements are summarized in Table 4.

(a) Influence of the Molar Mass of the Polymeric Core. The average particle size of gold and silver nanoparticles decreased with increasing M_w of the polymeric core (8.8 and 6.3 nm diameter for gold particles stabilized by PEI_5 and PEI_{21}, respectively, and 7.7 and 1.3 nm diameter for gold particles stabilized by PEI_5GLU and PEI_{21}GLU, respectively). Similar results were observed in the case dendrimer encapsulated nanoparticles.[44]

(b) Influence of the Substitution of Amino Groups. Functionalization of the amino groups with carbohydrate chains leads to nanoparticles with narrower size distribution and smaller mean particle diameter as compared to PEI_x (Figures 2 and 3). For example, in the case of PEI_{21}GLU, Ag and Au nanoparticles smaller than 2 nm were formed (1.9 and 1.4 nm diameter at ratios of 6 and 5, respectively) as compared to unfunctionalized PEI_{21} (10.8 and 6.3 nm diameter at ratios of 6 and 5, respectively). In this case, the resulting particle sizes are comparable to the ones obtained with PAMAM dendrimers.[19,20,23,44] Moreover, the comparison

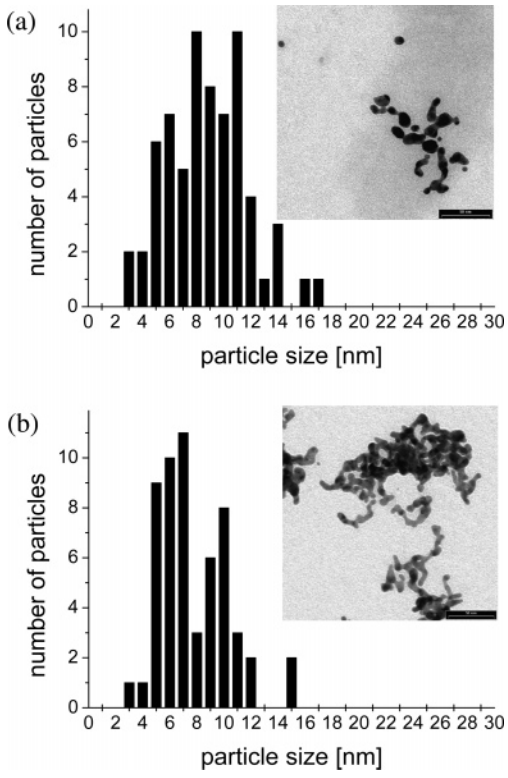

Figure 2. TEM histograms of Au particles of (a) PEI_5 after filtration (due to immediate partial precipitation after reduction) and (b) PEI_5GLU (without filtration, partial precipitation occurred after 1 week after reduction); mean diameter of PEI_5 and PEI_5GLU is 8.8 and 7.8 nm, respectively, at a ratio of [Au^{III}]/[polymer] of 6.8. Black bar in the TEM pictures equals 50 nm.

of the size of silver nanoparticles stabilized with three different polymers functionalized with carbohydrate chains (PEI_{25}GLU, PEI_{25}GLY, and PEI_{25}LAC) exhibited no significant differences (14, 13, and 13 nm, respectively, at a ratio of 25). It seems that the nature of the attached carbohydrate chain influences rather the stability properties than the particle size.

(c) Influence of the [Metal]/[Polymer] Ratio. It was reported in the literature that a Au^{III}/[G5.5]-PAMAM ratio of 10 (M_n [G5.5]-PAMAM = 50 864 g mol^{-1}) exhibited particle sizes of 5.6 nm, whereas at a ratio of 1/10 the synthesized particles were smaller (2.3 nm).[19] We have observed the same behavior and obtained smaller particle sizes after lowering the [metal ions]/[polymer] ratio. In the case of the PEI_{21}GLU the mean particle diameter of gold nanoparticles was 1.3 nm at a ratio of 5. A higher molecular weight PEI_{25}-

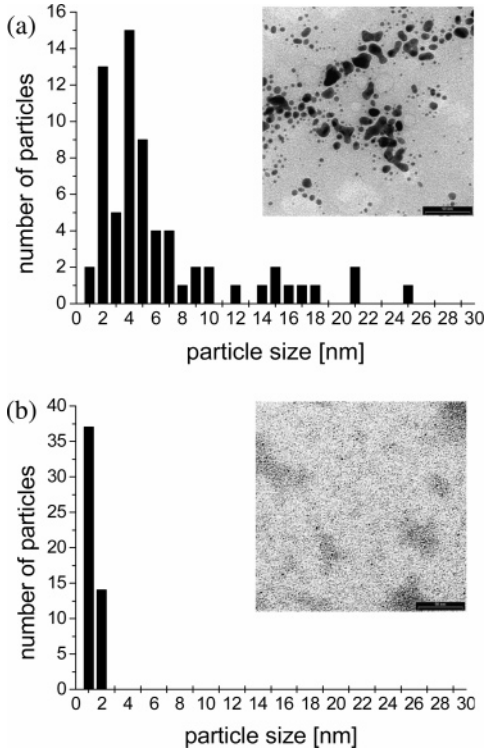

Figure 3. TEM histograms of Au particles of (a) PEI_{21} and (b) $PEI_{21}GLU$; mean diameter of PEI_{21} and $PEI_{21}GLU$ is 6.3 and 1.4 nm, respectively, at a ratio of $[Au^{III}]$/[polymer] of 5. Black bar in the TEM pictures equals 50 nm.

Scheme 2. Hydrogenation Reaction of Isophorone Catalyzed by Platinum Stabilized Nanoparticles

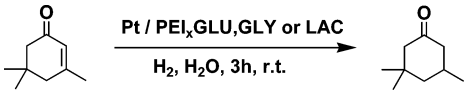

GLU led to a particle diameter of 4.1 nm at a ratio of 25. It is noteworthy that gold nanoparticles were much smaller than silver ones at the same ratio of 25 (4.2, 3.8, and 5.6 nm, respectively).

We were able to show that the dendritic architectures can be used as templates to obtain nanoparticles of defined size. In view of the observed cluster sizes and roughly estimating that the PEI_xGLU or PEI_x gyration radius is around 4.5 nm, a diameter of about 13 nm can only be explained if more than one macromolecule stabilizes a nanoparticle as suggested in the literature in the case of gold nanoparticles stabilized by low-generation PAMAM dendrimers.[19] However, high molecular weight polymers at low [metal ions]/[polymer] ratios (that leads to the smallest nanoparticles) might be able to stabilize nanoparticles in the interior of the polymer. Our studies demonstrate a clear template effect, i.e., the possibility to control the size of nanoparticles just by changing specific parameters: (i) molecular weight and functionalization and/or (ii) the [metal ions]/[polymer] ratio.

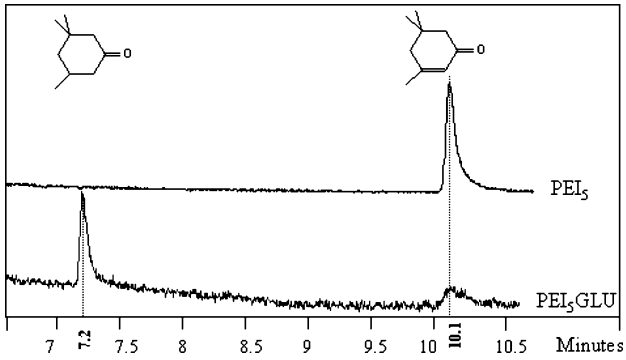

Figure 4. GC chromatograms of products of the hydrogenation reaction in the presence of PEI_5 and PEI_5GLU stabilized platinum nanoparticles for similar conditions (see Experimental Section).

Catalytical Applications. Oxidation of copper and silver nanoparticles (vide supra) has indicated the accessibility of the surface of metal nanoparticles and potential catalytic activity. As a first probe for the applicability of these polymer-stabilized water-soluble nanoparticles in catalysis, the hydrogenation of isophorone with hyperbranched polymer-encapsulated platinum nanoparticles was investigated in water under mild conditions (Scheme 2, low pressure of $H_2 = 2$ bar, room temperature). The product of the hydrogenation reaction was analyzed by monitoring the disappearance of isophorone by gas chromatography (commercial products were used as standards). Conversion rate was measured as well as the turnover number (TONs) defined as the moles of isophorone consumed by moles of Pt and the turnover frequencies (TOFs) defined as the moles of isophorone consumed by moles of Pt and by hour. The hydrogenation activities of nanoparticles stabilized by PEI_5, PEI_{25}, PEI_5GLU, $PEI_{25}GLU$, $PEI_{25}GLY$, and $PEI_{25}LAC$ are given in Table 5 as well as the ones of PAMAM of third and fourth generation ([G3]-PAMAM and [G4]-PAMAM, respectively) measured under the same conditions for comparison.

Catalytic activities for the chosen substrate isophorone are quite low, but in good agreement with the literature[45] considering the mild conditions that were used here. Moreover, they are calculated with respect to the entire amount of Pt present in the clusters; i.e., activity of the significant surface atoms will be higher. Nevertheless, the results obtained allow to describe the main characteristics of the catalytic activity of our systems. No reduction of the ketone function is observed. The only product resulting from hydrogenation is 3,3,5-

Table 5. Results Concerning Hydrogenation of Isophorone Catalyzed by Platinum-Stabilized Nanoparticles

	$[Pt^{IV}]$/[polymer]	stability	conversion [%]	TON[c]	TOF[c,d]
[G3]-PAMAM	20	stable	46.0	23.0	2.9
[G4]-PAMAM	20	stable	50.0	25.0	3.1
PEI_5	20	partial precipitation[a]	0.2	0.1	<0.1
PEI_5GLU	20	stable[b]	64.0	32.0	4.0
PEI_{25}	20	partial precipitation[a]	0.2	0.1	<0.1
$PEI_{25}GLU$	20	stable[b]	0.6	0.3	<0.1
$PEI_{25}GLY$	20	partial precipitation[a]	0.2	0.1	<0.1
$PEI_{25}LAC$	20	stable[b]	17.0	8.5	0.4

[a] Observed immediately. [b] Stable during the time of experiment; however, partial precipitation was observed after several weeks. [c] Calculated with respect to the entire amount of Pt present in the clusters; i.e., activity of the significant surface atoms will be higher. [d] Moles of isophorone consumed by moles of Pt and by hour (mol of isophorone (mol of Pt)$^{-1}$ h^{-1}).

trimethylcyclohexan-1-one. As expected, no significant catalytic activity was observed for systems that are not stable on the time scale of the experiment (PEI_5, PEI_{25}, $PEI_{25}GLY$): existence of large clusters not dispersed in aqueous solutions induced a decrease of the Pt surface accessible to the substrate and therefore poor catalytic activity. The catalytic activities of PEI_5GLU are comparable to [G3]-PAMAM and [G4]-PAMAM encapsulated platinum nanoclusters and demonstrate good accessibility of the colloidal metal for the substrate. The hydrogenation activity could be controlled in two ways. First, as already observed for dendrimers,[46] the hydrogenation reaction rate was lowered if a hyperbranched polymers with a high M_w was used (compare PEI_5GLU and $PEI_{25}GLU$) due to reduced accessibility of the substrates to the metal nanoparticles located in the interior of the polymer. In addition, modification of the outer shell (compare $PEI_{25}GLU$ and $PEI_{25}LAC$) allows a similar control. Very poor catalytic activities of $PEI_{25}GLY$ emphases the crucial role of stability for systems to be used as catalyst. After the hydrogenation reactions were run for up to 8 h, the solutions of stable nanoparticles remained clear, and there was no evidence of agglomeration (only after weeks partial precipitation occurred). The recycling of the catalyst (by ultracentrifugation and isolation as a powder) does not lead to a significant decrease in activity after redissolving it in water.

Conclusion

In summary, we have reported on a simple protocol to prepare dendritic core−shell architectures with carbohydrate shells. For the first time, hyperbranched PEI (polyethylenimine) or functionalized PEI with glycidol (PEI−GLY), gluconolactone (PEI−GLU), or lactobionic acid (PEI−LAC) molecules have been used as support materials for metal nanoparticles in water. Various parameters such as the concentration of the polymer in solution as well as the [metal ions]/[polymer] ratio and pH have been optimized. We were able to show that these dendritic polymers can act as colloid stabilizers to control the size of the nanoparticles. (In the case of $PEI_{21}GLU$ a template effect was clearly evidenced.) The attached carbohydrate shell influences rather the stability of the nanoparticles than their size. The preparation of these innovative materials involves anchory of Pt(IV) to the support prior to reduction with $NaBH_4$ in water. The TEM micrographs revealed that the dimensions of the clusters are greatly influenced by the nature of the polymeric stabilizer. The platinum nanoparticles stabilized with PEI derivatives proved to be as effective and robust for the selective hydrogenation of isophorone in water as the dendrimer derivatives. Moreover, they permit simple workup by phase separation, and the catalytical results demonstrate the ability to control the reaction rate by adjusting the chemical properties of the stabilizer (size of the core or nature of the shell). Furthermore, improvement of the biocompatibility induced by the carbohydrate shell will allow the additional usage of these particles in biological systems.

Experimental Section

GPC Measurement of PEI. GPC (gel permeation chromatography) of the PEIs have been performed by BASF AG with pullulan standard (Supporting Information). The molecular weights were confirmed by light scattering.

Attachment of Gluconolactone to PEI_x To Obtain PEI_xGLU. For example, PEI_{21} (1 g, 16.2 mmol g^{-1} T and L units), gluconolactone (1.466 g, 8.23 mmol), and stoichiometrical amounts of water (142 mg, 7.89 mmol) were mixed together and heated to 140 °C oil bath temperature for 10 min. About 50 wt % of the water was evaporated under these conditions to yield a light brown and brittle solid (yield: 99%). Inverse gated ^{13}C NMR (*d*-DMSO) revealed that about 30% of the gluconolactone is bonded via a salt bridge. IR: $\tilde{\nu}$ (cm^{-1}) = 1640 (C═O, covalent), 1600 (C═O, ionic). ^1H NMR (300 MHz, D_2O): δ (ppm) = 2.3−2.9 [m, *PEI*−CH_2−NHCO−CHOH−$(CHOH)_3$−CH_2OH], 3.2−3.3 [m, PEI−C*H*$_2$−NHCO−CHOH−$(CHOH)_3$−CH_2OH], 3.5−3.8 [m, PEI−CH_2−NHCO−CHOH−$(CHOH)_3$−CH_2OH], 3.8−4.0 [m, PEI−CH_2−NHCO−CHOH−$(CHOH)_3$−C*H*$_2$OH], 4.19 [s, PEI−CH_2−NHCO−C*H*OH−$(CHOH)_3$−CH_2OH]. ^{13}C NMR (75.4 MHz, D_2O): δ (ppm) = 38.7, 39.5, 40.4, 41.0 [PEI−*C*H_2−NHCO−$(CHOH)_4$−CH_2OH], 47.8, 49.6, 53.2, 54.7 [*PEI*−CH_2−NHCO−$(CHOH)_4$−CH_2OH], 65.0 [PEI−CH_2−NHCO−$(CHOH)_4$−*C*H_2OH], 72.7, 73.5, 74.5, 74.9, 75.8, 76.4 [PEI−CH_2−NHCO−(*C*H$O)_4$−CH_2OH], 176.7 [PEI−CH_2−NH*C*O−$(CHOH)_4$−CH_2OH], 180.9 [PEI−CH_2−NH_4^+ $^-$OO*C*−$(CHOH)_4$−CH_2OH]. Elemental analysis (found): C, 44.27%; N, 12.02%; H, 8.07%.

Attachment of Lactobionic Acid to PEI_{25} To Obtain $PEI_{25}LAC$. A solution of PEI_{25} (500 mg, 15.8 mmol g^{-1} T and L units) and lactobionic acid (1.423 g, 3.97 mmol) in water (12 mL) was adjusted to pH = 5 with hydrochloric acid, and 1-ethyl-3-[3-(dimethylamino)propyl]carbodiimide hydrochloride (EDC, 776.5 mg, 4.05 mmol) was added at room temperature. The reaction mixture was stirred for 3 days at room temperature. The crude product was dialyzed in water to obtain a yellow powder (yield: 69%). About 50% of lactobionic acid is covalently bonded according to inverse gated ^{13}C NMR. ^1H NMR (300 MHz, D_2O): δ (ppm) = 2.4−3.4 [*PEI*−C*H*$_2$−NHCO−lact], 3.4−4.5 [PEI−CH_2−NHCO-*lact*]. ^{13}C NMR (75.4 MHz, D_2O): δ (ppm) = 36.2, 37.4, 39.0 [PEI−*C*H_2−NHCO−lact], 45−55 [*PEI*−CH_2−NHCO−lact], 61.6, 62.4 [PEI−CH_2−NHCO−lact(*C*H_2OH)], 69.1, 70.8, 71.6, 72.2, 73.0, 75.8 [PEI−CH_2−NHCO−*lact*], 81.3, 82.1 [PEI−CH_2−NHCO−lact(*C*H−O−C(acetal)−O−*C*H)], 103.9 [PEI−CH_2−NHCO−lact(acetal-*C*)], 174.8, 175.8 [PEI−CH_2−NH*C*O−lact], 179.0 [PEI−CH_2−NH_4^+−OO*C*−lact]. Elemental analysis: N, 8.91%; C, 39.89%; H, 7.46%.

Attachment of DL-Glycidol to PEI_{25} To Obtain PEI_{25}-GLY. To a solution of PEI_{25} (1.0 g, 23.3 mmol g^{-1} N−H) in methanol (10 mL) a solution of DL-glycidol (11.7 mmol for 50% functionalization) in methanol (10 mL) was added in a dropwise fashion at room temperature. The reaction mixture was stirred for 1 day. Subsequent removal of the solvent yielded a colorless viscous oil (yield: 96%). ^1H NMR (300 MHz, D_2O): δ (ppm) = 2.5−2.8 [*PEI*−C*H*$_2$−CHOH−CH_2OH], 3.35 (traces of C*H*$_3$OH), 3.55 [PEI−CH_2−CHOH−C*H*$_2$OH], 3.82 [PEI−CH_2−C*H*OH−CH_2OH]. ^{13}C NMR (75.4 MHz, D_2O): δ (ppm) = 40−60 [*PEI*−*C*H_2−CHOH−CH_2OH], 49.3 (traces of *C*H_3OH), 64.5 [PEI−CH_2−CHOH−*C*H_2OH], 69.8, 70.8 [PEI−CH_2−*C*HOH−CH_2OH].

Typical Procedure for the Complexation Studies. For these experiments no buffered solutions were used. The solutions were equilibrated for at least 1 h before measurement.

Typical Procedure for the Hydrogenation of Isophorone with Platinum Nanoparticles. 10 mL of an aqueous solution containing 2×10^{-4} mol of H_2PtCl_6 complexed with 10^{-5} mol of $PEI_{25}GLU$ reduced by a 10-fold excess of $NaBH_4$ (relative to Pt) was stirred under H_2 for 1 h prior to the addition of 10^{-2} mol of isophorone. The progress of the reaction was followed by sampling at different time and extracting these samples with dichloromethane. The reaction product was analyzed by gas chromatography.

Gas chromatography measurements were performed with Varian Chrompack (CP-3800) apparatus equipped with a SGE nonpolar capillary column (BPX5 30 m × 0.25 mm) (injector temperature: 280 °C; splitless injection mode; carrier gas: helium at 1 mL min^{-1}; initial oven temperature: 60 °C, 1 min; rate 1: 20 °C min^{-1}; final temperature: 100 °C; rate 2: 20 °C min^{-1}; final temperature: 250 °C, 2 min; detector: 300 °C; solvent: dichloromethane). The retention time were found to

be ~10 min for the isophorone and 6.9 min for the corresponding hydrogened product.

Supporting Information Available: Experimental section consisting of figures showing NMR and IR spectra, calculation of the degree of functionalization of the polymers discussed, TEM micrographs, UV−vis data, GPC graphs and table with characteristics of PEI polymers, table illustrating stability of nanoparticles. This material is available free of charge via the Internet at http://pubs.acs.org.

References and Notes

(1) Scott, R. W. J.; Wilson, O. M.; Crooks, R. M. *J. Phys. Chem. B* **2005**, *109*, 692−704.
(2) Crooks, R. M.; Zhao, M.; Sun, L.; Chechik, V.; Yeung, L. K. *Acc. Chem. Res.* **2001**, *34*, 181−190.
(3) Maye, M. M.; Lou, Y.; Zhong, C.-J. *Langmuir* **2000**, *16*, 7520−7523.
(4) Cuenya, B. R.; Baeck, S.-H.; Jaramillo, T. F.; McFarland, E. W. *J. Am. Chem. Soc.* **2003**, *125*, 12928−12934.
(5) Jaramillo, T. F.; Baeck, S.-H.; Cuenya, B. R.; McFarland, E. W. *J. Am. Chem. Soc.* **2003**, *125*, 7148−7149.
(6) Hall, S. R.; Shenton, W.; Engelhardt, H.; Mann, S. *ChemPhysChem* **2001**, *3*, 184−186.
(7) Daniel, M.-C.; Astruc, D. *Chem. Rev.* **2004**, *104*, 293−346.
(8) Zheng, J.; Dickson, R. M. *J. Am. Chem. Soc.* **2002**, *124*, 13982−13983.
(9) Tkachenko, A. G.; Xie, H.; Coleman, D.; Glomm, W.; Ryan, J.; Anderson, M. F.; Franzen, S.; Feldheim, D. L. *J. Am. Chem. Soc.* **2003**, *125*, 4700−4701.
(10) Kim, Y.; Johnson, R. C.; Hupp, J. T. *Nano Lett.* **2001**, *1*, 165−167.
(11) Dragnea, B.; Chen, C.; Kwak, E.-S.; Stein, B.; Kao, C. C. *J. Am. Chem. Soc.* **2003**, *125*, 6374−6375.
(12) Donners, J. J. J. M.; Hoogenboom, R.; Schenning, A. P. H. J.; van Hal, P. A.; Nolte, R. J. M.; Meijer, E. W.; Sommerdijk, N. A. J. M. *Langmuir* **2002**, *18*, 2571−2576.
(13) Lewis, L. N. *Chem. Rev.* **1993**, *93*, 2693−2730.
(14) Kiwi, J.; Grätzel, M. *J. Am. Chem. Soc.* **1979**, *101*, 7214−7217.
(15) Sidorov, S. N.; Bronstein, L. M.; Valetsky, P. M.; Hartmann, J.; Cölfen, H.; Schnablegger, H.; Antonietti, M. *J. Colloid Interface Sci.* **1999**, *212*, 197−211.
(16) Bronstein, L. M.; Sidorov, S. N.; Gourkova, A. Y.; Valetsky, P. M.; Hartmann, J.; Breulmann, M.; Cölfen, H.; Antonietti, M. *Inorg. Chim. Acta* **1998**, *280*, 348−354.
(17) Zhou, Y.; Wang, C. Y.; Zhu, Y. R.; Chen, Z. Y. *Chem. Mater.* **1999**, *11*, 2310−2312.
(18) Mandal, M.; Ghosh, S. K.; Kundu, S.; Esumi, K.; Pal, T. *Langmuir* **2002**, *18*, 7792−7797.
(19) Esumi, K.; Kameo, A.; Suzuki, A.; Torigoe, K. *Colloids Surf. A: Physiochem. Eng. Aspects* **2001**, *189*, 155−161.
(20) Esumi, K.; Torigoe, K. *Prog. Colloid Polym. Sci.* **2001**, *117*, 80−87.
(21) Zhao, M.; Sun, L.; Crooks, R. M. *J. Am. Chem. Soc.* **1998**, *120*, 4877−4878.
(22) Balogh, L.; Tomalia, D. A. *J. Am. Chem. Soc.* **1998**, *120*, 7355−7356.
(23) Esumi, K.; Suzuki, A.; Aihara, N.; Usui, K.; Torigoe, K. *Langmuir* **1998**, *14*, 3157−3159.
(24) Li, Y.; El-Sayed, M. A. *J. Phys. Chem. B* **2001**, *105*, 8938−8943.
(25) Rahim, E. H.; Kamounah, F. S.; Frederiksen, J.; Christensen, J. B. *Nano Lett.* **2001**, *1*, 499−501.
(26) Ooe, M.; Murata, M.; Mizugaki, T.; Ebitani, K.; Kaneda, K. *Nano Lett.* **2002**, *2*, 999−1002.
(27) Fréchet, J. M. J.; Henmi, M.; Gitsov, I.; Aoshima, S.; Leduc, M. R.; Grubbs, R. B. *Science* **1995**, *269*, 1080−1083.
(28) Frey, H.; Haag, R. In *Encyclopedia of Materials, Science and Technology*; Buschow, K. H. J., R. H. C., Flemings, M. C., Ilschner, B., Kramer, E. J., Majahan, S., Eds.; Elsevier Science Ltd.: Oxford, 2001; pp 3997−4000.
(29) Aymonier, C.; Schlotterbeck, U.; Antonietti, L.; Zacharias, P.; Thomann, R.; Tiller, J. C.; Mecking, S. *Chem. Commun.* **2002**, 3018−3019.
(30) Mecking, S.; Thomann, R.; Frey, H.; Sunder, A. *Macromolecules* **2000**, *33*, 3958−3960.
(31) Sablong, R.; Schlotterbeck, U.; Vogt, D.; Mecking, S. *Adv. Synth. Catal.* **2003**, *345*, 333−336.
(32) Pérignon, N.; Mingotaud, A.-F.; Marty, J.-D.; Rico-Lattes, I.; Mingotaud, C. *Chem. Mater.* **2004.**
(33) Haag, R.; Krämer, M.; Stumbé, J.-F.; Krause, S.; Komp, A.; Prokhorova, S. *Polym. Prepr.* **2002**, *43*, 328.
(34) Garcia-Bernabé, A.; Krämer, M.; Oläh, B.; Haag, R. *Chem.—Eur. J.* **2004**, *10*, 2822−2830.
(35) Griessbach, R.; Meier, E.; Wassenegger, H. Farbenindustrie, I. G. US 2,223,930, 1940.
(36) Steuerle, U.; Reuther, W.; Harder, W. AG, B. WO 97/21760, 1997.
(37) Dick, C. R.; Potter, J. L.; Coker, W. P. Chemical, D. US 3,565,941, 1968.
(38) Hölter, D.; Frey, H. *Acta Polym.* **1997**, *48*, 298−309.
(39) Schmitzer, A.; Perez, E.; Rico-Lattes, I.; Lattes, A.; Rosca, S. *Langmuir* **1999**, *15*, 4397−4403.
(40) Schmitzer, A. R.; Franceschi, S.; Perez, E.; Rico-Lattes, I.; Lattes, A.; Thion, L.; Erard, M.; Vidal, C. *J. Am. Chem. Soc.* **2001**, *123*, 5956−5961.
(41) Yonezawa, Y.; Kawabata, I.; Sato, T. *Ber. Bunsen-Ges. Phys. Chem.* **1996**, *100*, 39.
(42) Zheng, J.; Stevenson, M. S.; Hikida, R. S.; van Patten, P. G. *J. Phys. Chem. B* **2002**, *106*, 1252−1255.
(43) Turkevich, T.; Stevenson, P. C.; Hillier, J. *Discuss. Faraday Soc.* **1951**, *11*, 55−75.
(44) Esumi, K.; Suzuki, A.; Yamahira, A.; Torigoe, K. *Langmuir* **2000**, *16*, 2604−2608.
(45) Sipos, E.; Tungler, A.; Bitter, I. *J. Mol. Catal. A* **2003**, *198*, 167−173.
(46) Wells, M.; Crooks, R. M. *J. Am. Chem. Soc.* **1996**, *118*, 3988−3989.

MA0510791